The impact of metallicity and X-rays on star formation

Marco Spaans[1], Aycin Aykutalp[1], Seyit Hocuk[1]

[1]Kapteyn Astronomical Institute, University of Groningen,
P.O. Box 800, 9700 AV Groningen, the Netherlands
email: spaans@astro.rug.nl

Abstract. Star formation is regulated through a variety of feedback processes. In this study, we treat feedback by metal injection and a UV background as well as by X-ray irradiation. Our aim is to investigate whether star formation is significantly affected when the ISM of a proto-galaxxy enjoys different metallicities and when a star forming cloud resides in the vicinity of a strong X-ray source. We perform cosmological Enzo simulations with a detailed treatment of non-zero metallicity chemistry and thermal balance. We also perform FLASH simulations with embedded Lagrangian sink particles of a collapsing molecular cloud near a massive, 10^7 $M_\odot$, black hole that produces X-ray radiation.

We find that a multi-phase ISM forms for metallicites as small as 10^{-4} Solar at $z = 6$, with higher ($10^{-2} Z_\odot$) metallicities supporting a cold (< 100 K) and dense ($> 10^3$ cm^{-3}) phase at higher ($z = 20$) redshift. A star formation recipe based on the presence of a cold dense phase leads to a self-regulating mode in the presence of supernova and radiation feedback. We also find that when there is strong X-ray feedback a collapsing cloud fragments into larger clumps whereby fewer but more massive protostellar cores are formed. This is a consequence of the higher Jeans mass in the warm (50 K, due to ionization heating) molecular gas. Accretion processes dominate the mass function and a near-flat, non-Salpeter IMF results.

**Keywords.** stars: formation — hydrodynamics — chemistry — IMF

1. Brief Context

The presence of metals and X-rays in star forming regions affect processes like gas heating, ionization degree and cooling time, and do so up to column densities of 10^{24} cm^{-2} that are typical of dense cores (e.g., Hocuk & Spaans 2010; Meijerink & Spaans 2005). At the same time, star formation in the early universe and inside active galactic nuclei may depend strongly on the ambient metallicity and radiation background as well as on mechanical feedback from supernovae (e.g., Greif *et al.* 2010).

2. Low-Metallicity Halos at High Redshift

In the Enzo simulations we use 128^3 grid cells on the top grid with three nested subgrids, each refining by a factor of two. The box size of the simulations is 1-8 Mpc/h and a concordance cosmology is adopted. We run simulations from redshift 99 to 5 for a pre-enriched ISM, using different cooling prescriptions for metallicities of 10^{-4}, 10^{-3}, 10^{-2} and 10^{-1} Solar. In these simulations, we have used a star formation recipe which derives from the metallicity dependent ISM phase structure and we include UV radiation and supernova feedback from PopIII stars. The metallicity dependent cooling is computed with the Meijerink & Spaans (2005) UV chemistry code and includes fine-structure emissions from carbon and oxygen as well as molecular lines from species like

507
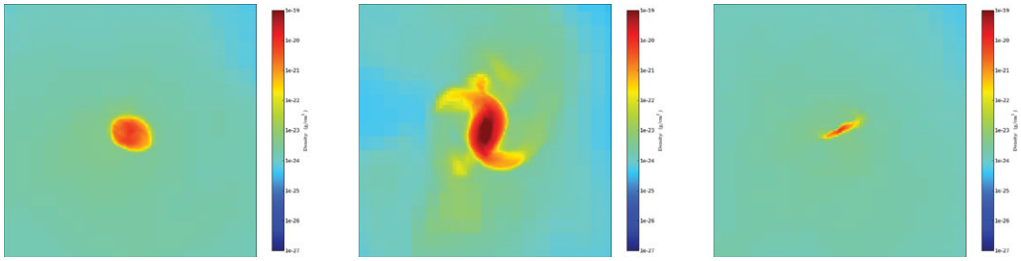
Figure 1. Density profiles of a minihalo at $z \approx 5.4$ for metallicities of $Z/Z_\odot = 10^{-4}$ (left), $Z/Z_\odot = 10^{-2}$ (middle), and $Z/Z_\odot = 10^{-2}$ with a $J_b = 100J_{-21}$ radiation field (right).
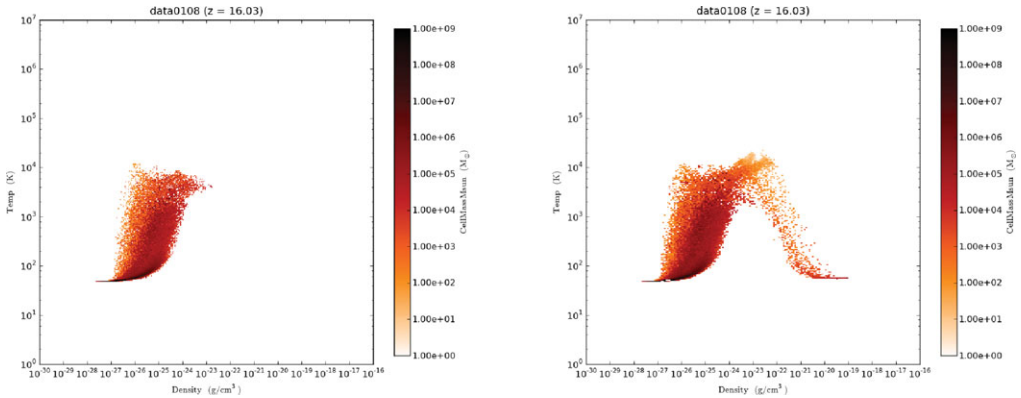
**Figure 2.** Density-temperature phase diagrams at $z \approx 16$ for $Z/Z_\odot = 10^{-4}$ (left) and $Z/Z_\odot = 10^{-2}$ (right).

H$_2$, CO and water. Heating is provided by adiabatic compression, dust grain photo-electric emission and supernovae. All level populations are computed under statistical equilibrium. The chemistry includes gas phase and grain surface formation of H$_2$ and HD (Cazaux & Spaans 2004, 2009). CPU demands prevent global radiation transfer to be performed. Instead, we work with a precomputed grid of cooling rates that augment the zero metallicity rates already present in Enzo.

A multi-phase ISM develops, at various times, once the metallicity exceeds a value of about 10^{-4} Solar, consistent with Jappsen *et al.* (2009). The key feature in this is the presence of a cold (< 100 K) and dense ($> 10^3$ cm^{-3}) phase. The redshift at which a multi-phase ISM is established depends on the metallicity, see figure 2 for $z \approx 16$. Also, the $Z/Z_\odot = 10^{-2}$ case evolves faster dynamically compared to the $Z/Z_\odot = 10^{-4}$ case due to the shorter cooling time. The higher metallicity halo is more compact and although mergers are more violent it recovers faster than the $Z/Z_\odot = 10^{-4}$ case (see figure 1, left two panels). In a run where we switch to $Z/Z_\odot = 10^{-1}$ at redshift 12 we first form more stars due to a stronger presence of a cold dense phase. Consequently, the minihalo experiences severe feedback effects. Due to the efficient cooling ability of the metal-rich gas, the halo maintains its density structure but the cold dense phase is largely destroyed (see figure 3).

As a first attempt to include the effects of UV radiation feedback, we have performed runs with a constant background radiation field of magnitude equal to the mean Galactic value (about $J_b = 100J_{-21}$). This background dissociates molecules like CO completely and leaves little H$_2$ despite the self-shielding ability of the latter. It should be emphasized that J_b is merely chosen and that the transfer of radiation is strictly local. Still, these first
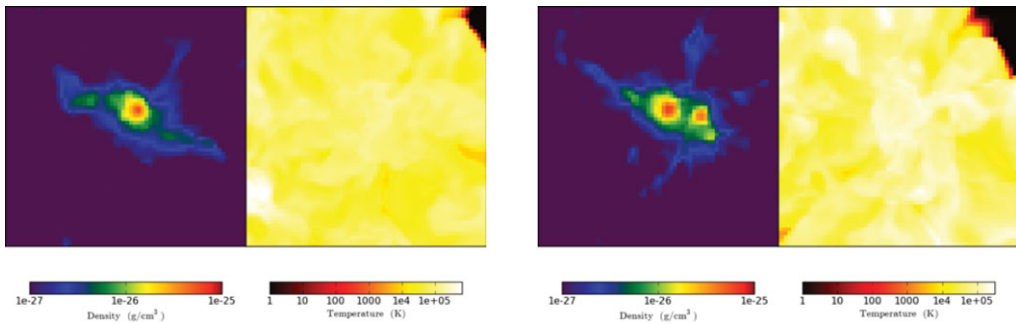
Figure 3. Density-temperature slices at $z \approx 6$, for star formation and feedback on runs. Shown are a constant $Z/Z_\odot = 10^{-2}$ run (left) and one for which $Z/Z_\odot$ jumps from 10^{-2} to 10^{-1} at $z = 12$ (right).
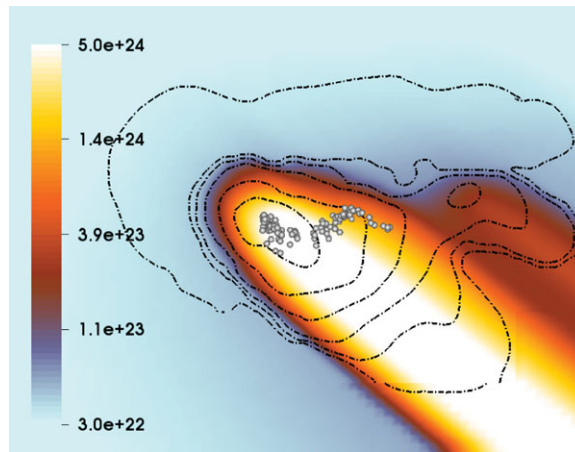

Figure 4. Column density (cm^{-2}) slice of a molecular cloud under the impact of X-rays (at $t = t_{\text{ff}}$). The colors represent the column density along the line of sight to the black hole, which is located at the upper left side. The density is shown in black contours. Contour levels are 1, 4, 16, 64, 256, 1024 $\times 10^4$ cm^{-3}. The white spheres indicate the locations of the protostars.

calculations do indicate that the cold dense phase is fragile for metallicities of $Z/Z_\odot \leqslant 10^{-2}$ (figure 1, right panel). In all, supernova and radiation feedback act to diminish the presence of a cold dense phase (at a given metallicity) and thus allow self-regulation for a star formation recipe that is based on a cold and dense phase.

3. X-ray Irradiation of a Cloud near a Black Hole

In order to follow the effects caused by X-rays on the temperature of the gas, the X-ray chemistry code of Meijerink & Spaans (2005) is ported into FLASH. This code again includes all relevant atomic and molecular cooling lines and carefully treats secondary ionizations by fast electrons, Coulomb heating and ion-molecule/neutral-neutral reactions. Given an X-ray flux, gas density, and global column density along the line of sight to the source, the code calculates the temperature and chemical abundances self-consistently. This output is fed into the simulation at every iteration yielding a complete X-ray chemistry extension of FLASH. The cloud is located at 10 pc from the black hole. A k^{-4} turbulent spectrum is imposed as well as Keplerian shear. The initial cloud mass is 800 M$_\odot$. The X-ray flux is 160 erg s^{-1} cm^{-2} with an $E^{-0.9}$ power-law distribution
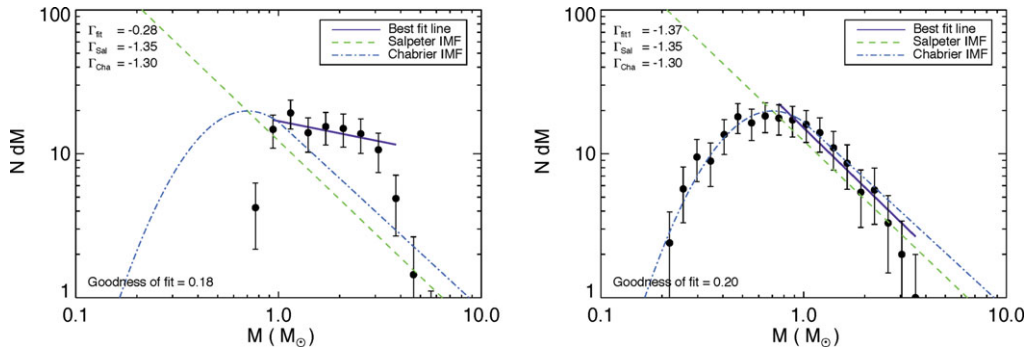
Figure 5. The IMF of two simulations at $t = t_{ff}$. Left panel shows the IMF for the simulation with X-rays, and the right panel shows the IMF for the simulation without X-rays.

between 1 and 100 keV. Sink particles are implemented following Federrath *et al.* (2010) and Krumholz *et al.* (2004).

X-rays heat the cloud from one side, where the accreting black hole is located. This increases the thermal pressure and causes the outer gas layers to expand and evaporate. At the same time, the molecular cloud is compressed as an ionizing pressure flow travels inwards. Finger-like shapes are formed, with a high density head, and the gas that is lying in their shadows is well shielded, see figure 4. The increased density and external thermal pressure, caused the efficient ($\sim 30\%$) ionization heating, then induces star formation.

The simulation with X-rays results in a much flatter IMF slope than the one without radiation, $\Gamma_{X-ray} = -0.28$ after 10^5 years of evolution (see figure 5). This is much flatter than the Salpeter slope of -1.35 that we find for the simulation without X-rays, which has a typical cloud temperature of 10 K due to cosmic ray heating only. These trends are maintained at higher dynamical times, $t = 2t_{ff}$. The main reason for the change in IMF comes from the Jeans mass. The efficient X-ray heating yields temperatures in the cloud of 50 K at densities as high 10^6 cm^{-3} and columns of 10^{23-24} cm^{-2}. We find that the sink particles still grow in mass after $2t_{ff}$ and experience competitive accretion.

References

Cazaux, S. & Spaans, M. 2004, *ApJ*, 611, 40
Cazaux, S. & Spaans, M. 2009, *A&A*, 496, 365
Federrath., C., Banerjee, R., Clark, P. C., & Klessen, R. S. 2010, *ApJ*, 713, 269
Greif, T. M., Glover, S. C. O., Bromm, V., & Klessen, R. S. 2010, *ApJ*, 716, 510
Hocuk, S. & Spaans, M. 2010, *A&A*, 510, A110
Jappsen, A.-K., Klessen, R. S., Glover, S. C. O., & Mac Low, M.-M. 2009, *ApJ*, 696, 1065
Krumholz, M. R., McKee, C. F., & Klein, R. I. 2004, *ApJ*, 611, 399
Meijerink, R. & Spaans, M. 2005, *A&A*, 436, 397